

This article was downloaded by:

On: 25 January 2011

Access details: *Access Details: Free Access*

Publisher *Taylor & Francis*

Informa Ltd Registered in England and Wales Registered Number: 1072954 Registered office: Mortimer House, 37-41 Mortimer Street, London W1T 3JH, UK



Separation Science and Technology

Publication details, including instructions for authors and subscription information:

<http://www.informaworld.com/smpp/title~content=t713708471>

PARAMETRIC SENSITIVITY ANALYSIS OF DIRECT CONTACT MEMBRANE DISTILLATION

Fahmi A. Abu Al-Rub^a; Fawzi Banat^a; Khalid Beni-Melhim^b

^a Chemical and Petroleum Engineering Department, United Arab Emirates University, Al-Ain, United Arab Emirates ^b Potash Arab Company, Kerak, Jordan

Online publication date: 10 September 2002

To cite this Article Al-Rub, Fahmi A. Abu , Banat, Fawzi and Beni-Melhim, Khalid(2002) 'PARAMETRIC SENSITIVITY ANALYSIS OF DIRECT CONTACT MEMBRANE DISTILLATION', *Separation Science and Technology*, 37: 14, 3245 — 3271

To link to this Article: DOI: 10.1081/SS-120006160

URL: <http://dx.doi.org/10.1081/SS-120006160>

PLEASE SCROLL DOWN FOR ARTICLE

Full terms and conditions of use: <http://www.informaworld.com/terms-and-conditions-of-access.pdf>

This article may be used for research, teaching and private study purposes. Any substantial or systematic reproduction, re-distribution, re-selling, loan or sub-licensing, systematic supply or distribution in any form to anyone is expressly forbidden.

The publisher does not give any warranty express or implied or make any representation that the contents will be complete or accurate or up to date. The accuracy of any instructions, formulae and drug doses should be independently verified with primary sources. The publisher shall not be liable for any loss, actions, claims, proceedings, demand or costs or damages whatsoever or howsoever caused arising directly or indirectly in connection with or arising out of the use of this material.



SEPARATION SCIENCE AND TECHNOLOGY, 37(14), 3245–3271 (2002)

PARAMETRIC SENSITIVITY ANALYSIS OF DIRECT CONTACT MEMBRANE DISTILLATION

**Fahmi A. Abu Al-Rub,^{1,*} Fawzi Banat,²
and Khalid Beni-Melhim³**

¹Chemical and Petroleum Engineering Department,
United Arab Emirates University, P.O. Box 17555, Al-Ain,
United Arab Emirates

²Department of Chemical Engineering, Bahrain University,
Al-Manamah, Bahrain

³Potash Arab Company, Kerak, Jordan

ABSTRACT

Membrane distillation is a thermally driven mass transfer in which a porous hydrophobic membrane separates two liquid phases and a temperature difference is maintained as the driving force. In this study, the technique of direct contact membrane distillation (DCMD) process, where the liquid phases are in direct contact with both sides of the membrane, has been investigated for the case of pure water production. Parametric sensitivity analysis and temperature polarization factor are used to study the sensitivity of the mass flux to the different parameters associated with DCMD for water production, and the effect of these parameters on the thermal efficiency of the DCMD process has been investigated.

*Corresponding author. Fax: +971-3-762-4262; E-mail: f.rub@uaeu.ac.ae

The results obtained show that the mass flux of pure water production is highly sensitive to the feed bulk temperature, and at low flow rates of hot and cold fluids, to the heat transfer coefficients. Results also show that increasing membrane thickness decreases the mass flux of pure water and decreases temperature polarization effect. In addition, results show that temperature polarization effect becomes significant as feed bulk temperature increases.

Key Words: Membrane distillation; Sensitivity; Direct contact; Flux

INTRODUCTION

Membrane distillation (MD) is a relatively new separation process which depends on using porous hydrophobic membranes to immobilize a liquid–vapor interface at the pore entrance. In direct contact membrane distillation (DCMD), the oldest type of the MD processes, the membrane is in contact with liquid phase on evaporation and condensation sides of the membrane, which are kept at different temperatures while a gaseous phase, usually air, is entrapped within the membrane pores, as shown in Fig. 1. Due to the temperature difference across the membrane sides, a diffusion process through the membrane occurs.

Several theoretical and experimental studies have been published on DCMD process. Findley^[1] was the first researcher who suggested the concept of MD process. He suggested that if a suitable hydrophobic membrane material, which stands high temperatures and with long life can be obtained, a new economical process for evaporation can be achieved.

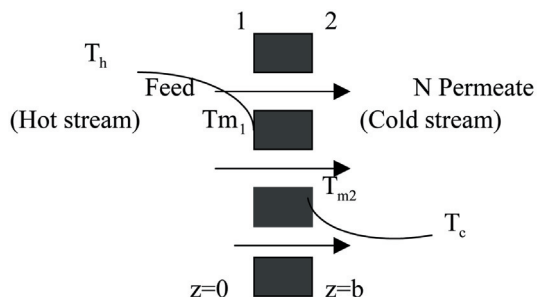


Figure 1. Principle of DCMD.



Gostoli and Sarti^[2] studied experimentally and theoretically the DCMD system for aqueous solutions containing ethanol. They analyzed the relevant process parameters on the separation factor. They suggested the use of air gap membrane distillation (AGMD) instead of DCMD in order to prevent the possible membrane wetting by ethanol which may occur on the permeate side.

Cheng^[3] and Cheng and Wiersma^[4] suggested the use of a composite membrane in which a hydrophilic layer is coated on the top of a hydrophobic microporous membrane. The purpose of this design was to prevent membrane wetting that could be caused by crystal growth of salt through membrane pores.

Sarti et al.^[5] studied theoretically and experimentally, the MD process for water desalination process. It was found that the comparison between model predictions and experimental data was quite satisfactory when the heat transfer coefficient is known with high accuracy in the hot stream.

Sarti and Gostoli,^[6] Sarti et al.,^[7] and Gostoli and Sarti^[8] used the DCMD as well as AGMD configurations for the production of pure water from salt solutions using polytetrafluoroethylene (PTFE) membranes. Their main consideration was to examine the relationship between the temperature difference between the hot and cold side and the permeate flux. Although relevant mathematical models were presented, no accurate quantitative description was achieved. They attributed this to the possible effects of the process heat transfer coefficient.

Fane et al.^[9] studied theoretically the transport process in MD process. The theoretical study was used to analyze pilot plant data and optimize the design of larger scale systems. It was found that under some conditions, MD is competitive with reverse osmosis for production of distilled or potable water for industrial or arid-zone use.

Banat et al.^[10–12] investigated the use of MD in breaking the azeotropic point of aqueous mixtures. They showed that MD can shift the azeotropic point of some aqueous mixtures. Banat et al.^[13] studied theoretically the simultaneous removal of acetone and ethanol from aqueous solutions using MD by applying the Fickian and Stefan-Maxwell approaches. Abu Al-Rub et al.^[14] investigated theoretically the removal of dilute acetone from aqueous streams using MD by applying the Fickian and Stefan-Maxwell relations.

Bandini et al.^[15] were the first group who studied the effect of different variables on the efficiency of DCMD. They used the dimensionless sensitivity approach to study the sensitivity of the total flux in DCMD to heat and mass transfer coefficients, the only two parameters studied. Banat et al.^[16] extended this approach to analyze the sensitivity of the total flux to all parameters involved in vacuum membrane distillation.

In this study, the sensitivity of the total flux to all parameters associated in DCMD will be investigated using the dimensionless sensitivity approach. In addition, other two approaches, namely, temperature polarization factor (TPF) and thermal efficiency will be studied in detail. The analysis will be



applied to the case of pure water production, which simulates the desalination application.

THEORY

Model Description for Mass and Heat Transfer Across Gas Membrane

Mass Transfer

Let us consider two streams kept at different temperatures and separated by a gas membrane as shown in Fig. 1. At steady state, the molar flux of water vapor (N) diffusing through a stagnant air film is given by^[17]

$$N = -\frac{cD}{1-y} \frac{dy}{dz} \quad (1)$$

where y is the mole fraction of water and c is the molar density. Equation (1) is based on the assumption that the molecular diffusion is the prevailing mechanism of mass transport.

According to the ideal gas law

$$c = \frac{P}{RT_{av}} \quad (2)$$

where T_{av} is the average temperature between condensation and evaporation surfaces.

Equation (1) can be integrated at steady state conditions with the following boundary conditions:

$$z = 0 \quad y = y_1 \quad (3)$$

$$z = b \quad y = y_2 \quad (4)$$

then the molar flux will be

$$N = \frac{DP}{bRT_{av}} \frac{(P_1^* - P_2^*)}{P_{C,lm}^*} \quad (5)$$

where b is the membrane thickness, P^* , the partial pressure of water vapor, and $P_{C,lm}^*$ is the log mean partial pressure difference of the stagnant compound defined as:

$$P_{C,lm}^* = \frac{P_{c2}^* - P_{c1}^*}{\ln \frac{P_{c2}^*}{P_{c1}^*}} \quad (6)$$



To account for the membrane porosity (ϵ) and tortuosity (τ), the effective molar flux will be

$$N_{\text{eff}} = \frac{\epsilon}{\tau} N \quad (7)$$

Therefore:

$$N_{\text{eff}} = \frac{\epsilon}{\tau bRT_{\text{av}}} \frac{(P_1^* - P_2^*)}{P_{C,\text{lm}}^*} \quad (8)$$

A typical value for membrane tortuosity (τ) equals 2^[5] which was used in all the calculations.

Theoretical study of Eq. (8) requires a knowledge of the interfacial temperatures T_{m1} and T_{m2} as shown in Fig. 1, thus heat balance across the membrane is required.

Heat Transfer

At steady state, the heat transfer rate from the feed bulk to the membrane surface at which evaporation starts is equal to the heat transfer rate through the membrane and this equals the heat transfer rate from the other side of the membrane to the coolant fluid (see Fig. 1). Heat transfer through the membrane involves heat transfer through the membrane matrix and pores plus the heat of evaporation at the feed side of the membrane.

The heat transfer from the bulk feed to the membrane surface is given by:

$$q = h_b(T_b - T_{m1}) \quad (9)$$

where T_b is the feed bulk temperature, T_{m1} , the interfacial temperature at the hot side of the membrane, and h_b is the hot side heat transfer coefficient. Heat transfer through the membrane is given by:

$$q = \frac{K_m}{b} (T_{m1} - T_{m2}) + \lambda N + NC_{pg}(T_{m1} - T_{m2}) \quad (10)$$

where K_m , the thermal conductivity of the composite material of air and material of the membrane, is given by the following equation:

$$K_m = k_s(1 - \epsilon) + k_{\text{air}}\epsilon \quad (11)$$

T_{m2} is the interfacial temperature at the cold side of the membrane and C_{pg} is the specific heat of the water vapor. The first term of Eq. (10) represents the heat conduction across the membrane and the term $N\lambda$ represents the latent heat of evaporation (diffusion heat). The third term which represents the sensible heat is negligible in comparison with the other two terms.

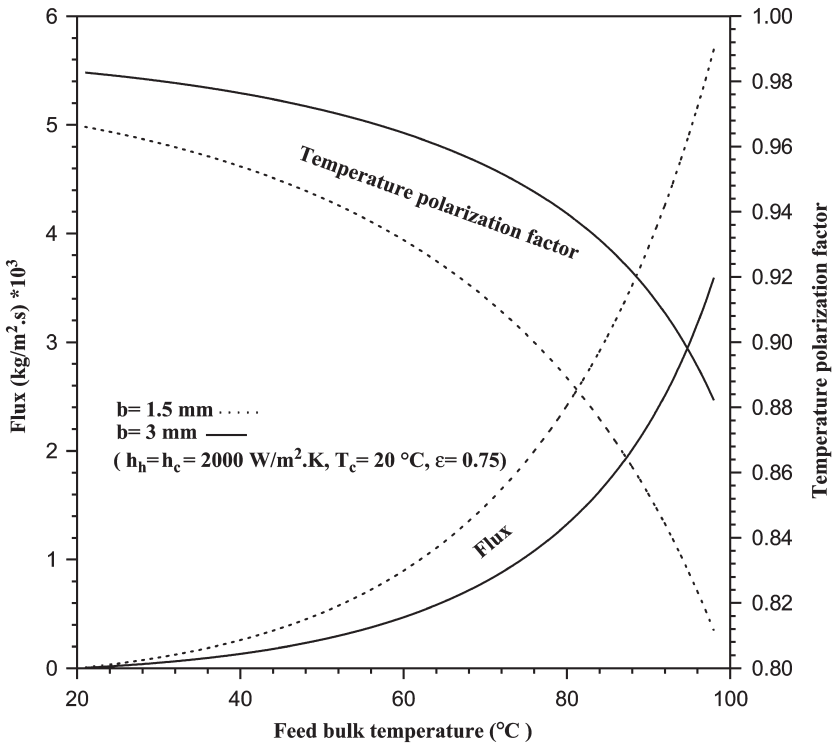


Figure 2. Effect of feed bulk temperature on mass flux and TPF.

The heat transfer from the cold side of the membrane to the coolant fluid is given by:

$$q = h_c(T_{m2} - T_c) \quad (12)$$

where T_c is the coolant temperature and h_c is the cold side heat transfer coefficient. Equations (9), (10), and (12) can be solved for the interfacial temperatures to give:

$$T_{m1} = \beta \left\{ \left(1 + \frac{K_m}{h_c b} \right) T_b + \frac{K_m}{h_h b} T_c - \frac{N\lambda}{h_h} \right\} \quad (13)$$

$$T_{m2} = \beta \left\{ \left(1 + \frac{K_m}{h_h b} \right) T_c + \frac{K_m}{h_c b} T_b + \frac{N\lambda}{h_c} \right\} \quad (14)$$

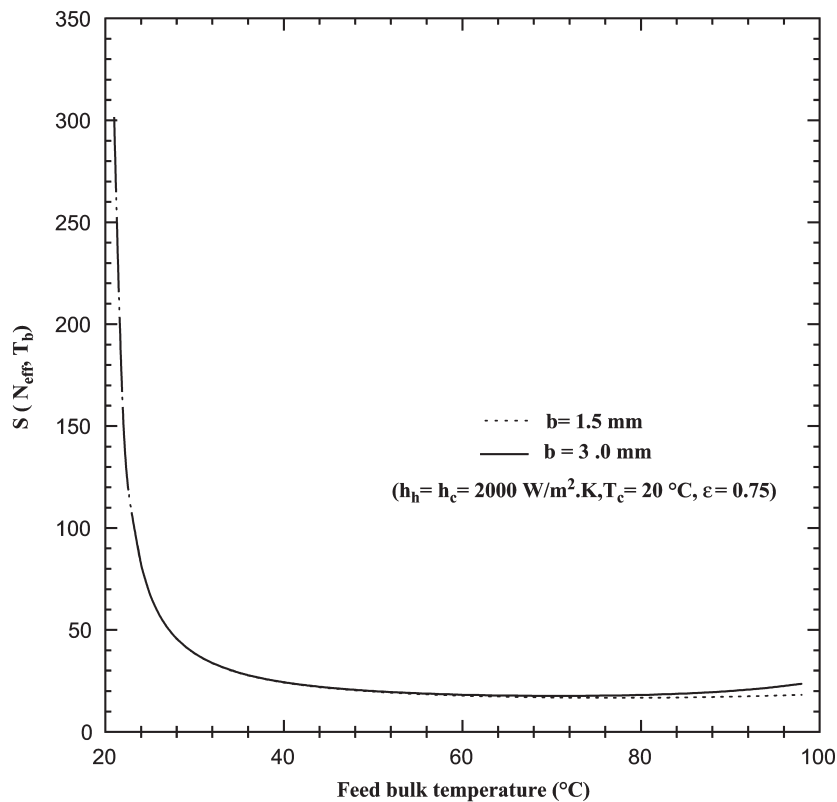


Figure 3. Response of (N_{eff}, T_b) to feed bulk temperature.

where:

$$\beta = \frac{1}{\left(1 + \frac{K_m}{bh_h} + \frac{K_m}{bh_c}\right)} \quad (15)$$

The dependence of diffusivity on temperature and concentration was taken into consideration using the equation:

$$cD = 6.3 \times 10^{-5} \sqrt{T} \quad (16)$$

which is based on experimental diffusion in water vapor-air mixtures at temperatures around 40°C.

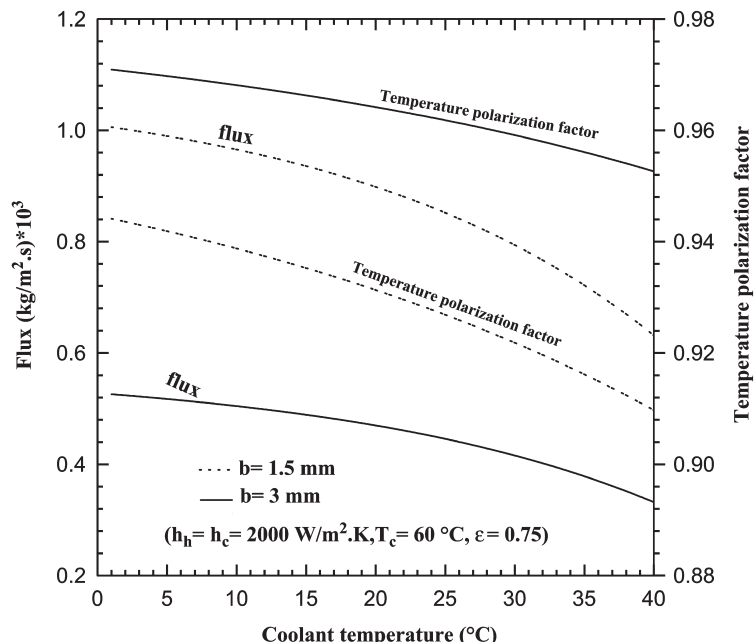


Figure 4. Effect of coolant temperature on mass flux and TPF.

Parametric Sensitivity Study

Parametric sensitivity analysis (PSA) plays an important role in determining the sensitivity of different parameters in any mathematical model. In any mathematical model, there are input parameters that affect the response of the output variables. A parameter is considered sensitive if a small change in its value produces a large change in the output variable. A sensitive parameter may be considered as a “valuable”; which maximizes a favorable output response, or a “noise” parameter; which minimizes a favorable output response or maximizes unfavorable output response. Knowing these parameters is essential in evaluating the economics of any process or operation. In the case of MD processes, it is very important to maximize the mass flux of some components in the feed. Thus, PSA can be used as a tool to investigate the effect of the different parameters associated in these processes on the mass flux.

In order to study the effect of the different parameters on the mass flux of pure water system in DCMD, the following two approaches will be discussed:

1. Temperature polarization factor
2. Dimensionless sensitivity analysis method

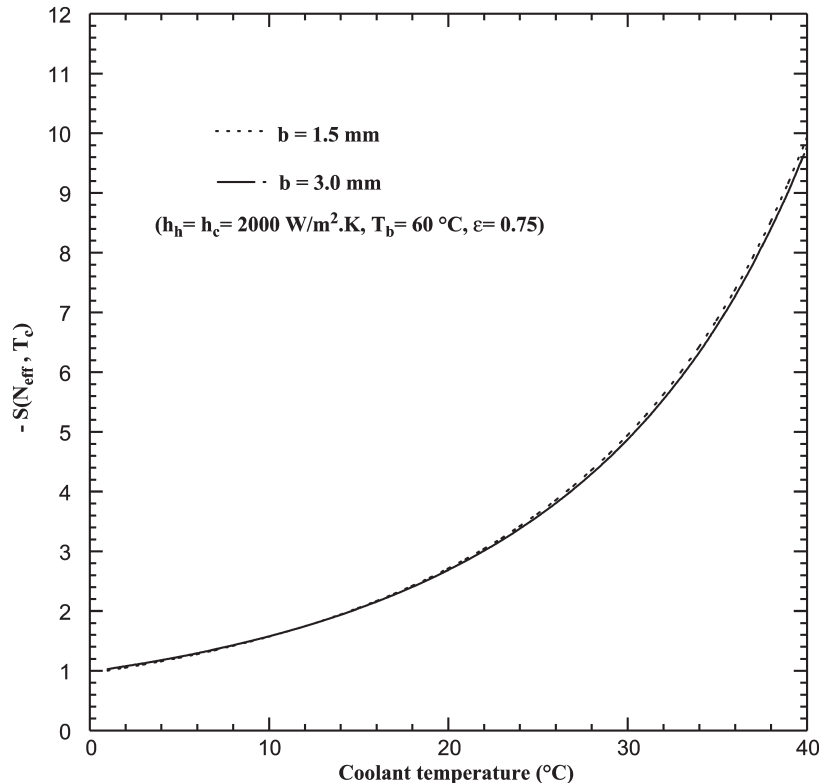


Figure 5. Response of (N_{eff}, T_c) to coolant temperature.

Temperature Polarization Factor (θ)

The temperature polarization phenomenon occurs as a result of temperature gradient across the membrane (see Fig. 1). This temperature gradient is due to the heat flux through the liquid layer, which is needed to provide the required heat for evaporation at the membrane interface. The temperature variation across the membrane can be related with each other by the TPF which is defined as:

$$\theta \equiv \frac{\Delta T_{\text{eff}}}{\Delta T_{\text{bulk}}} = \frac{T_{m1} - T_{m2}}{T_b - T_c} \quad (17)$$

The numerical values of θ lie within the range $[0-1]$. As $\theta \rightarrow 0.0$, $T_{m1} \rightarrow T_{m2}$ and thus the driving force across the membrane is negligible while as $\theta \rightarrow 1$,

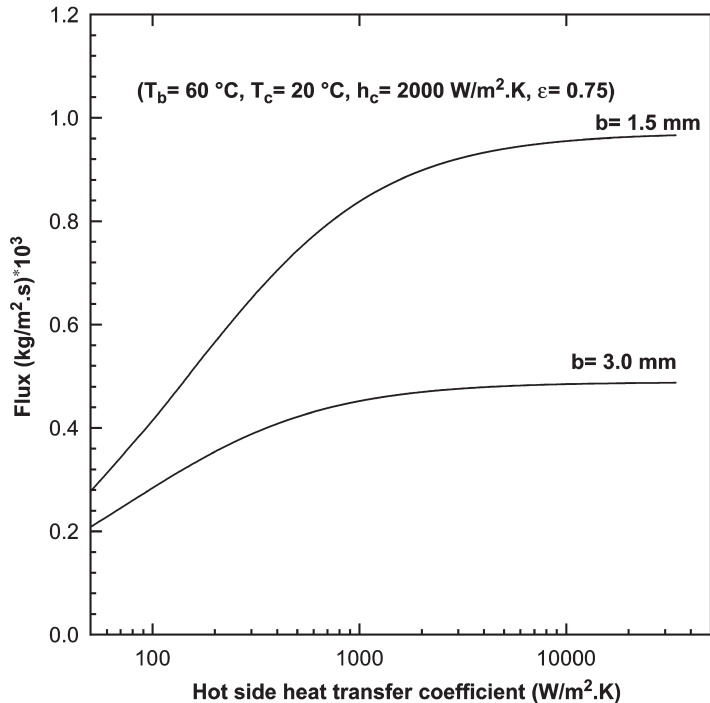


Figure 6. Effect of hot side heat transfer coefficient on mass flux.

the difference between the membrane interfacial temperatures ($T_{m1} - T_{m2}$) starts to approach the difference of the bulk temperatures, and thus the polarization effect is not significant.

Dimensionless Sensitivity Analysis Method

A dimensionless sensitivity factor, also called as normalized sensitivity factor, is defined as^[18]

$$S(R, P_i) \equiv \frac{\partial \ln R}{\partial \ln P_i} = \frac{P_i \partial R}{R \partial P_i} = s(R, P_i) \frac{P_i}{R} \quad (18)$$

where P_i is any parameter that may affect R . In the case of pure water, R represents the mass flux (N) and P_i may be any one of the input parameters affecting N , e.g. $\{T_b, T_c, h_h, h_c, b, \varepsilon\}$. As the studied parameters are not dimensionally homogeneous, normalized sensitivity factors provide a systematic and much convenient way to compare the effects of these parameters.

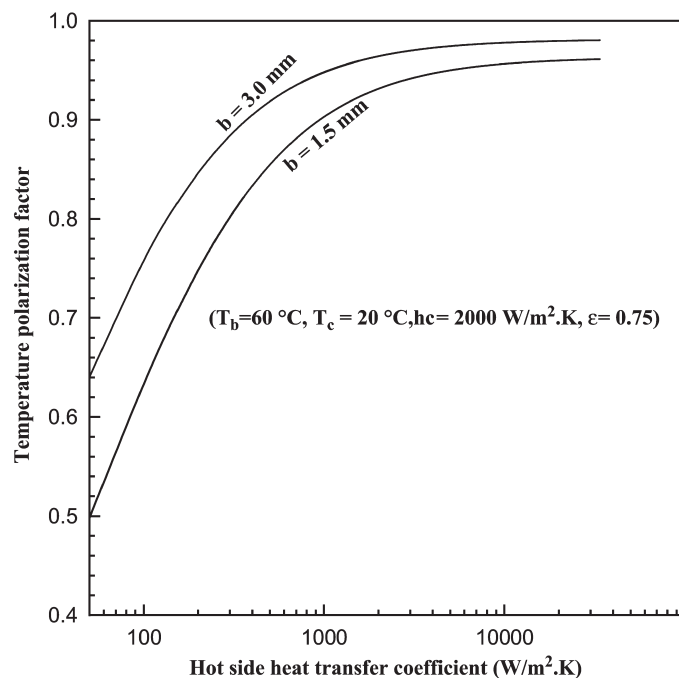


Figure 7. Effect of hot side heat transfer coefficient on TPF.

RESULTS AND DISCUSSION

In the following discussion, the symbol N in the $S(N, P_i)$ refers to the effective mass flux (N_{eff}) as it is indicated in the figures. Notice that because the input parameters P_i 's are related to the mass flux (N) by implicit relationship, the mass flux is calculated first and saved for each parameter. Then the saved data are used as an input to calculate the first derivatives numerically using central difference formulas.

Effect of the Feed Bulk Temperature

Figure 2 shows the effect of the variation of the feed bulk temperature on the mass flux with membrane thickness as a parameter. The polarization effect is also shown on the same figure. This figure shows that the mass flux increases exponentially by increasing the feed bulk temperature. This is due to the typical relationship between vapor pressure and temperature which is

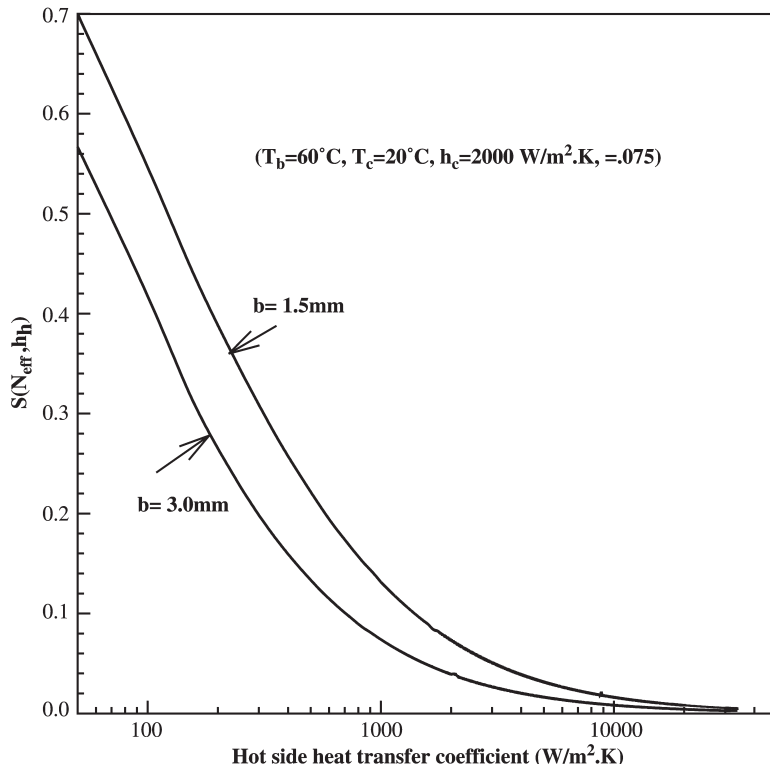


Figure 8. Response of (N_{eff}, h_h) to hot side heat transfer coefficient.

presented by the Antoine's equation. On the other hand, the mass flux decreases by increasing the membrane thickness; this is due to the increase in the mass transfer resistance.

In contrast to that, the polarization factor decreases by increasing the feed bulk temperature and increases by increasing the membrane thickness. An increase in feed temperature will increase the difference between T_b and T_c and also the difference between T_{m1} and T_{m2} . The increase in the difference $(T_{m1} - T_{m2})$ will be small in comparison with the increase in difference $(T_b - T_c)$, thus the net result is a decrease in TPF as can be shown by using Eq. (17). On the other hand, under given conditions, increasing the membrane thickness increases the resistance to heat transfer, thus increases the driving force for heat transfer for the same amount of heat to be transferred. Thus, increasing membrane thickness results in an increase in the difference between T_{m1} and T_{m2} and thus the polarization factor increases.

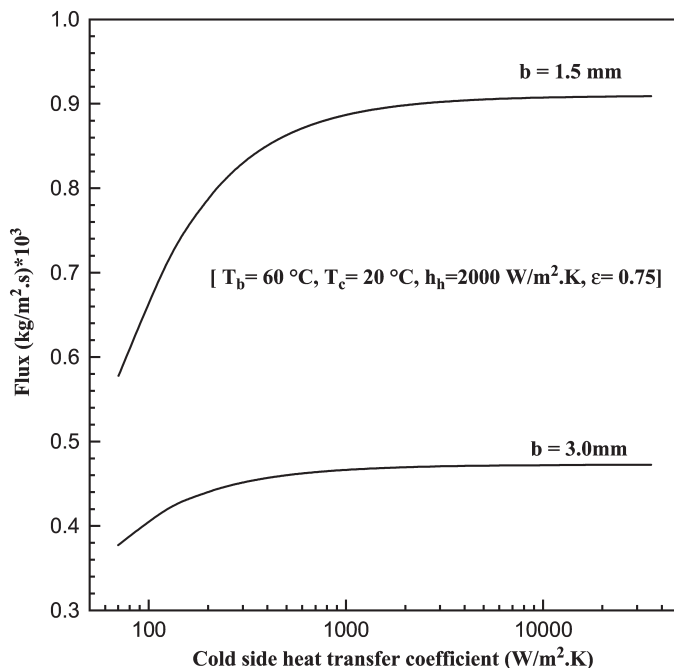


Figure 9. Effect of cold side heat transfer coefficient on mass flux.

The normalized sensitivity of the mass flux to T_b , $S(N, T_b)$, is shown in Fig. 3. It is noticed that the sensitivity factor $S(N, T_b)$ is always greater than one, which means that the percentage change in the transmembrane flux, due to a given change in the feed bulk temperature only, is always greater than the percentage which is considered for T_b . The sensitivity shows a sharp maximum at lower temperatures of T_b . This is due to the fact that at lower bulk temperatures (i.e., when $T_b \rightarrow T_c$), the driving force between T_b and T_c is at the minimum and any small change in T_b will highly affect the mass flux. On the other hand, and due to the exponent dependency of water vapor pressure on temperature, the sensitivity of the vapor pressure, and thus the mass flux is expected to be higher at higher temperatures. The results obtained in Fig. 3 suggest that the contribution of the sensitivity of driving force to temperature at lower temperatures is dominant over the sensitivity of the vapor pressure to feed temperature. Thus the net result is a decrease in $S(N, T_b)$ with the increase in T_b at lower temperatures. As the temperature increases, the contribution of the vapor pressure effect in the overall sensitivity of flux to T_b increases in the overall sensitivity of flux to T_b . Thus at higher temperature ($T_b > 60^{\circ}\text{C}$) the sensitivity is expected to be constant with increasing T_b .

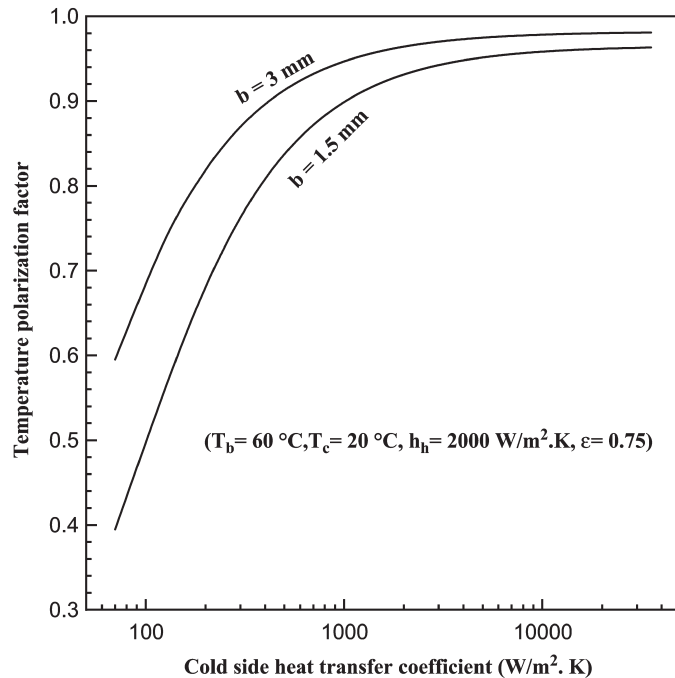


Figure 10. Effect of cold side heat transfer coefficient on TPF.

Finally it is observed from the figure that the sensitivity of the mass flux to the feed bulk temperature is not affected by varying the membrane thickness and only small effect is observed at higher temperatures.

Effect of the Coolant Temperature

In Fig. 4 the mass flux of pure water system as well as the polarization effect are plotted vs. the coolant temperature with the membrane thickness as a parameter. The results obtained show that the mass flux decreases by increasing the coolant temperature. This is due to the decrease in the driving force between the bulk temperatures which affects the actual driving force across the membrane, i.e., T_{m1} , and T_{m2} . The increase in the membrane thickness will decrease the mass flux by increasing the resistance to flow through the membrane. Figure 4 shows that the polarization factor decreases with increasing T_c . Increasing T_c results in a decrease in the difference between T_b and T_c , thus, this difference will result in an

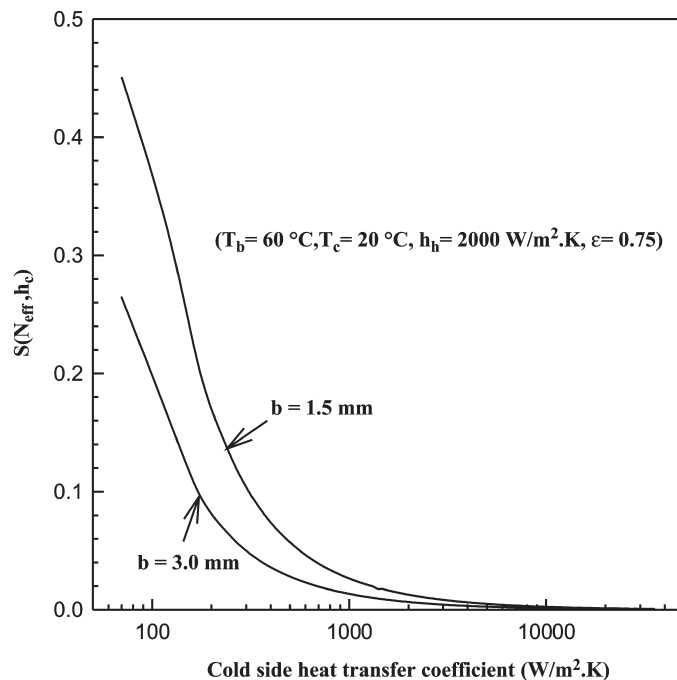


Figure 11. Response of (N_{eff}, h_c) to cold side heat transfer coefficient.

increase in the polarization factor as can be seen from the definition of the polarization factor. However, increasing T_c , also results in a decrease in the driving force across the membrane, i.e., $(T_{m1} - T_{m2})$ which will result in a decrease in the polarization factor. This decrease in the polarization factor is faster than the increase in the polarization factor due to the decrease in the difference between T_b and T_c ; resulting in an overall decrease in the polarization factor as T_c increases. This behavior is identical to the one obtained by TPF vs. T_b in Fig. 2. Thus, one can conclude that no real and direct conclusion can be obtained about the sensitivity parameters by using the polarization factor approach.

The sensitivity of the mass flux to the coolant temperature is shown in Fig. 5. This figure shows that the mass flux has less sensitivity at lower temperature values of T_c , and the sensitivity increases when $T_c \rightarrow T_b$. This conclusion is in agreement with the one obtained in Fig. 3, i.e., when $T_b \rightarrow T_c$; the system tends to be highly sensitive.

Moreover, the negative values of $S(N, T_c)$ are in agreement with the fact that the increase in T_c causes a decrease in the mass flux. And again, $S(N, T_c)$ is unaffected by the membrane thickness.

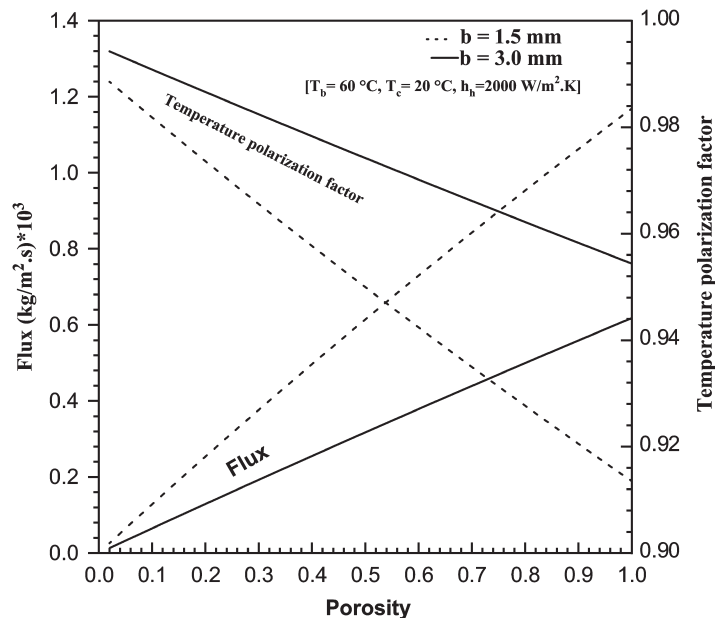


Figure 12. Effect of membrane porosity on mass flux and TPF.

Effect of the Hot Side Heat Transfer Coefficient

The effect of the hot side heat transfer coefficient on mass flux is shown in Fig. 6, and on the polarization effect is shown in Fig. 7. Figure 6 shows that the mass flux sharply increases at lower values of heat transfer coefficient in the hot side while the flux tends to be constant at very large values of h_h , the same trend is obtained for the polarization effect as shown in Fig. 7. As the heat transfer coefficient in the hot side increases, the surface temperature on the hot surface of the membrane side approaches the feed stream bulk temperature (i.e., $T_{m1} \rightarrow T_b$), then, the value of $(T_{m1} - T_{m2})$ will slightly increase, since the denominator $(T_b - T_c)$ is constant, the polarization effect increases. The effect of the membrane thickness on the TPF is also shown in the same figure, apparently as the membrane thickness increases, and by increasing h_h , the polarization factor approaches one.

Figure 8 shows the normalized sensitivity of the mass flux to hot side heat transfer coefficient, i.e., $S(N, h_h)$. The numerical values of the sensitivity factor are found to be within the range [0, 1]. The sensitivity of mass flux to the hot side heat transfer coefficient decreases with increasing h_h . The sensitivity of the mass flux to the hot side heat transfer coefficient is high at lower values of h_h , and it

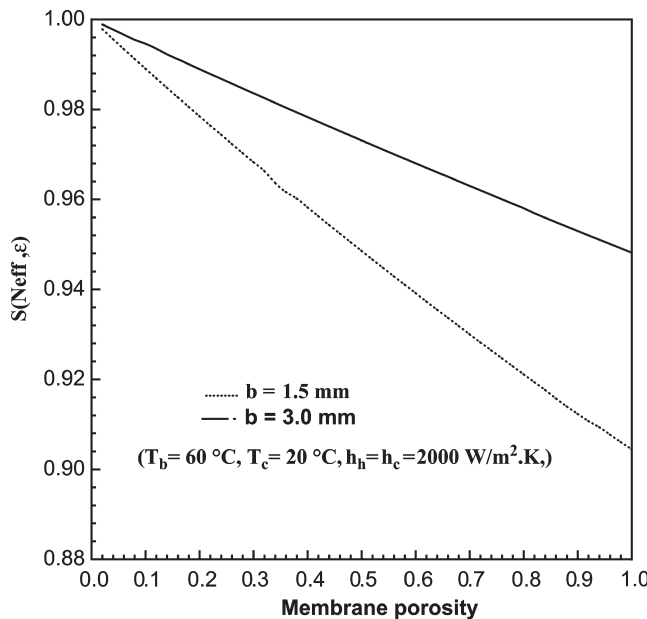


Figure 13. Response of $(N_{\text{eff}}, \varepsilon)$ to membrane porosity.

tends to approach zero when the heat transfer coefficient has higher values. This is in agreement with the fact that the flux is almost constant when $h \rightarrow \infty$.

Effect of the Cold Side Heat Transfer Coefficient

The effect of the cold side heat transfer coefficient on mass flux is shown in Fig. 9 with the membrane thickness as a parameter. This figure shows that the effect of cold side heat transfer on the mass flux is significant only at lower values of h_c . As it is shown from the figure, the effect is almost negligible when the membrane thickness increases. The polarization effect has the same trend as the mass flux, as shown in Fig. 10.

The normalized sensitivity of the mass flux to the cold side heat transfer coefficient is shown in Fig. 11. This figure shows that $S(N, h_c)$ decreases with increasing h_c , a behavior similar to that of $S(N, h_h)$. At higher values of h_c , $S(N, h_c) \rightarrow 0.0$, thus, the mass flux is not sensitive to h_c , and increasing h_c will provide no advantage to the process. This is due to the fact that at high values of h_c , the mass flux, as shown in Fig. 9 is not affected by h_c , thus $S(N, h_c) \rightarrow 0.0$.

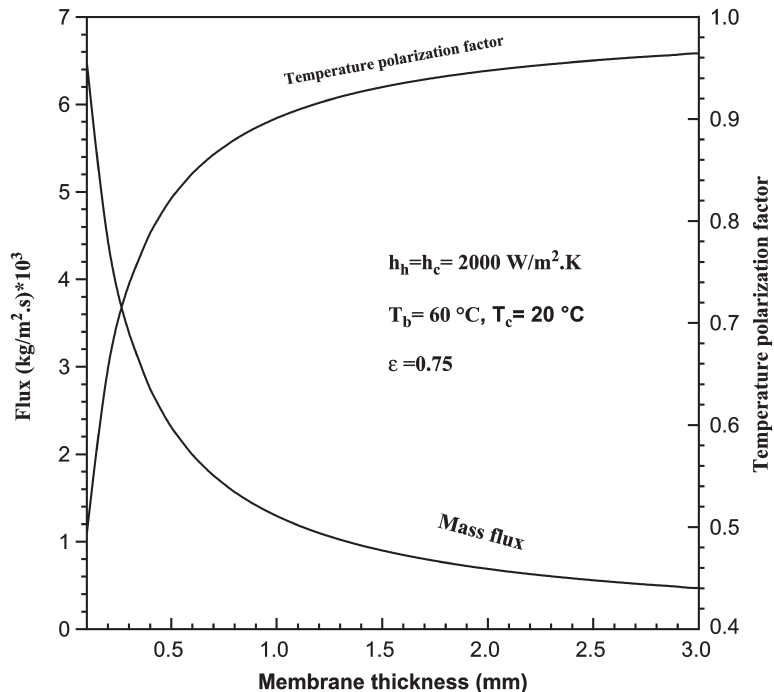


Figure 14. Effect of membrane thickness on mass flux and TPF.

Finally, under same conditions, $S(N, h_h) > S(N, h_c)$ and $S(N, h_h)$ approaches zero more rapidly than $S(N, h_c)$. This is obviously shown in Figs. 8 and 11. This means that the flux is more sensitive to hot side heat transfer coefficient than the cold under the same operating conditions.

Effect of Porosity

The variation of mass flux with porosity is shown in Fig. 12. The figure shows that the mass flux linearly increases with the porosity as expected from Eq. (8). On the other hand, the polarization factor, shown in the same figure, decreases by increasing the porosity. This is because as $\varepsilon \rightarrow 0.0$ there is no mass flux and $T_{m1} \rightarrow T_b$ and $T_{m2} \rightarrow T_c$ thus $\theta \rightarrow 1$.

The normalized sensitivity of mass flux to the membrane porosity, $S(N, \varepsilon)$, is shown in Fig. 13. The numerical values of $S(N, \varepsilon)$ are close to one, this is supported in Fig. 12 in which the variation of polarization factor with porosity is

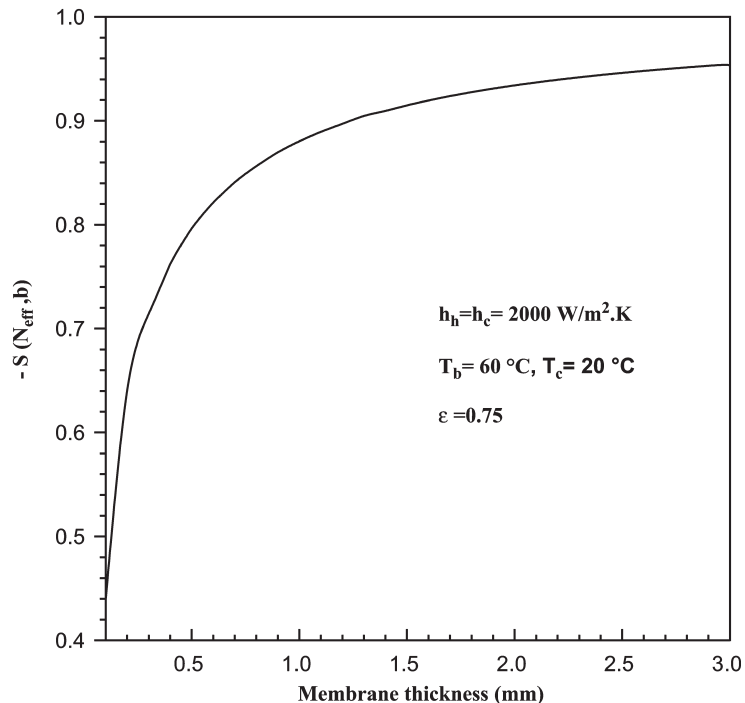


Figure 15. Response of (N_{eff}, b) to membrane thickness.

shown. As it is shown in the figure the polarization factor is close to one for the whole range of porosity, thus, $(T_{m1} - T_{m2}) \rightarrow (T_b - T_c)$, this means that the temperature polarization increases slightly with increasing the membrane porosity.

When $\varepsilon \rightarrow 0.0$, $\theta \rightarrow 1$, the case at which the sensitivity factor $S(N, \varepsilon)$ approaches unity as can be calculated from Eq. (8). And as the membrane thickness increases, the polarization factor approaches one, the case at which $(\Delta T_{\text{eff}} \rightarrow \Delta T_{\text{bulk}})$ or $(T_{m1} \rightarrow T_b)$ and $(T_{m2} \rightarrow T_c)$. This conclusion is supported by increasing the membrane thickness as shown in Fig. 13.

Effect of Membrane Thickness

The influence of the membrane thickness, discussed earlier, can be shown by considering the membrane thickness as the variation parameter. The

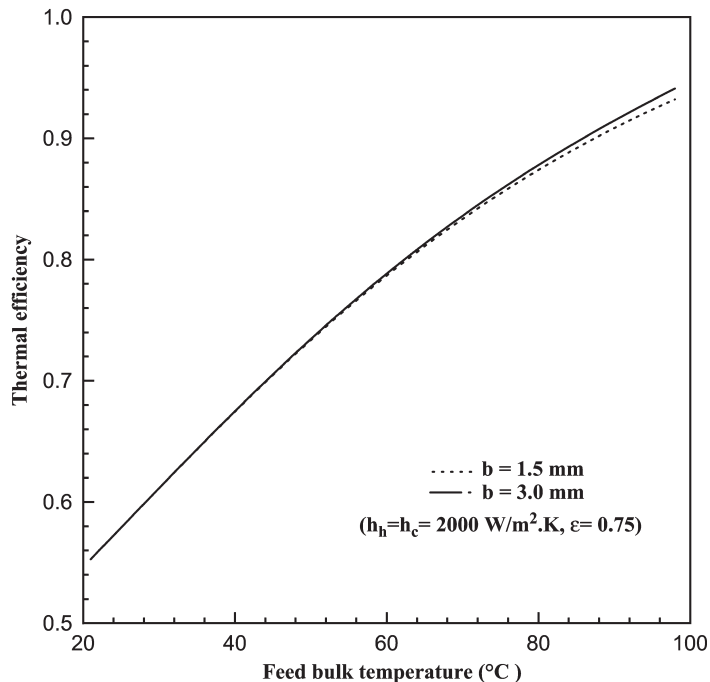


Figure 16. Effect of feed bulk temperature on thermal efficiency.

effect of the membrane thickness on mass flux and TPF is shown in Fig. 14. The mass flux is inversely proportional to the membrane thickness according to Eq. (8). Increasing the membrane thickness increases the diffusion path and this will increase the mass transfer resistance and thus decreases the flux. The polarization factor increases by increasing the membrane thickness. For large values of the membrane thickness, the thermal resistance of the gas membrane dominates and $(\Delta T_{\text{eff}} \rightarrow \Delta T_{\text{bulk}})$, i.e., $(T_{m1} - T_{m2}) \rightarrow (T_b - T_c)$ and so $\theta \rightarrow 1$.

Figure 15 shows the normalized sensitivity factor of mass flux to the membrane thickness. Apparently, the sensitivity factor has negative values which supports the fact that increasing the membrane thickness reduces the mass flux. This figure shows that the normalized sensitivity factor $S(N, b)$ increases (in negative) with increasing the thickness of the membrane. As shown, $S(N, b)$ approaches unity for thicker membrane which means a negligible mass flux as it is shown in Fig. 14.

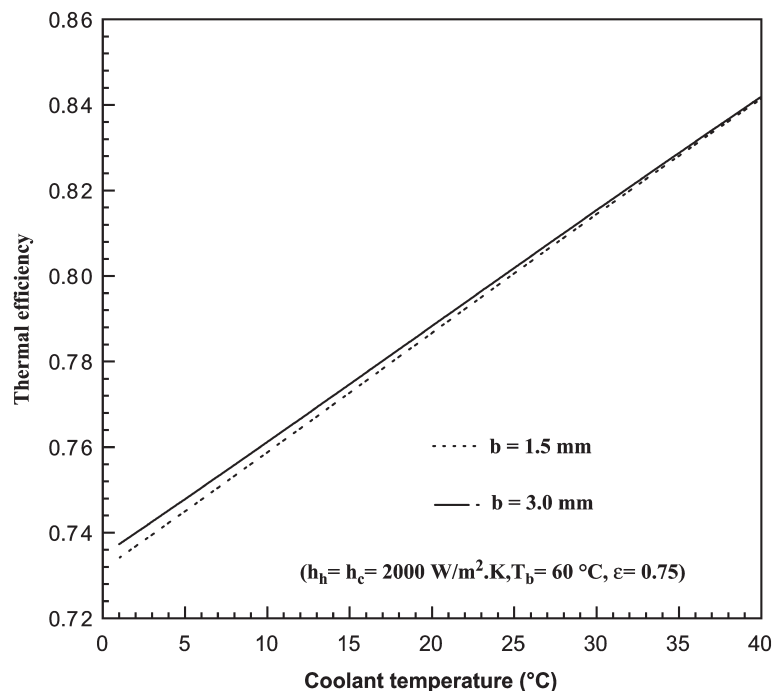


Figure 17. Effect of coolant temperature on thermal efficiency.

Thermal Efficiency of Membrane Distillation Process

The results obtained make it possible to estimate the sensitivity of mass flux to various input parameters. In practical applications of MD process, one of the most important and crucial issues is the MD efficiency, which determines cell design and, eventually, the operating parameters. This can be achieved simply by introducing the thermal efficiency of MD process, which is defined as the ratio of the heat used in evaporation to the total heat input to the module. The thermal efficiency of the DCMD can be defined by the following equation:

$$\eta = \frac{N\lambda}{\frac{K_m}{b}(T_{m1} - T_{m2}) + N\lambda} \quad (19)$$

Next, the effect of the relevant parameters on the thermal efficiency of DCMC will be discussed in detail.

In Fig. 16, the thermal efficiency of the process is shown as a function of the feed bulk temperature T_b . It is found that the thermal efficiency increases by

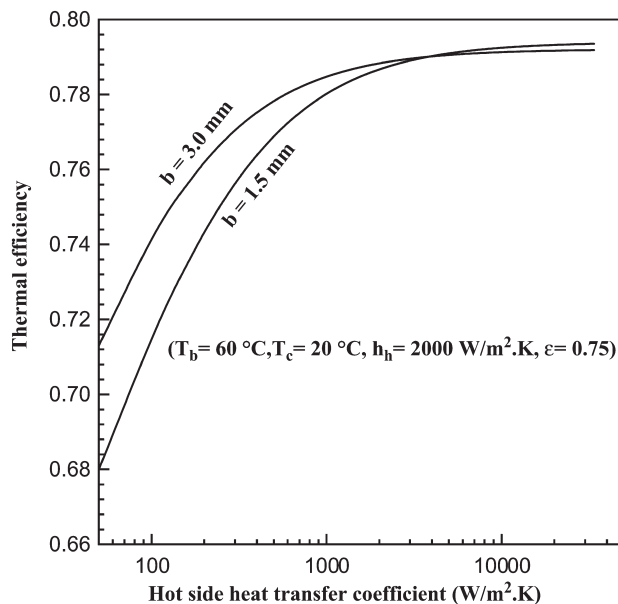


Figure 18. Effect of hot side heat transfer coefficient on thermal efficiency.

increasing the bulk temperature. The increase in the thermal efficiency of the process reflects the fact that the energy losses become less compared to the energy needed for evaporation at high feed bulk temperature.

Figure 16 shows that an increase in membrane thickness by 100% has no effect on the thermal efficiency. This is because increasing the membrane thickness leads to a decrease in both the heat of conduction through the membrane and the heat associated by evaporation in a counter balance manner.

The effect of coolant temperature on the thermal efficiency is shown in Fig. 17. The thermal efficiency increases by increasing the coolant temperature, this is due to the decrease in the heat losses by increasing T_c . Figure 17 shows that the effect of membrane thickness on the thermal efficiency is negligible due to the similar argument discussed previously.

The thermal efficiency as a function of hot side heat transfer coefficient is shown in Fig. 18. The thermal efficiency of the process has the same trend of mass flux and polarization factor as shown previously. Figure 18 shows that at lower values of h_h , the thermal efficiency is greater for the thicker membrane. This is because increasing h_h increases T_{m1} and therefore both the heat loss by conduction and heat transferred by evaporation are increased. However, because

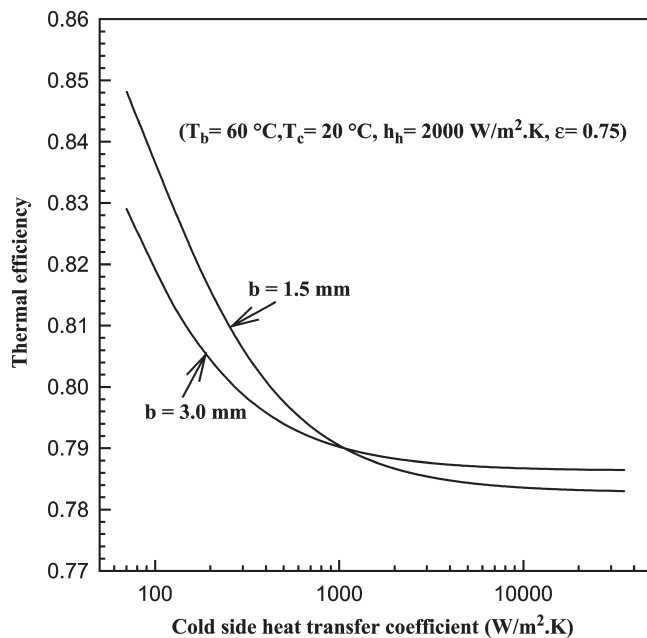


Figure 19. Effect of cold side heat transfer coefficient on thermal efficiency.

N is exponentially dependent on T_{m1} , any small change in T_{m1} will be reflected more on $N\lambda$ than the conduction term. On the other hand, at high values of h_b , the flux tends to be constant and N will be independent of h_b , the case at which the heat lost by conduction will overcome on the heat of diffusion and thus the net result is a decrease in the thermal efficiency for thicker membranes at high values of h_b .

The effect of the cold side heat transfer coefficient on the thermal efficiency of the process is shown in Fig. 19. The results show that the thermal efficiency decreases by increasing the cold side heat transfer coefficient. This is obvious from the definition of the thermal efficiency and the effect of h_c on N and $(T_{m1} - T_{m2})$.

The thermal efficiency of the process is shown as a function of the membrane porosity in Fig. 20. The thermal efficiency increases sharply at lower values of porosity but it tends to be constant as $\theta \rightarrow 1$. No effect is observed on the thermal efficiency by increasing the membrane thickness by 100%, the reason for that is the same as it was discussed for T_b and T_c .

Figure 21 shows that the effect of membrane thickness on thermal efficiency is almost negligible. This is due to the reason discussed earlier.

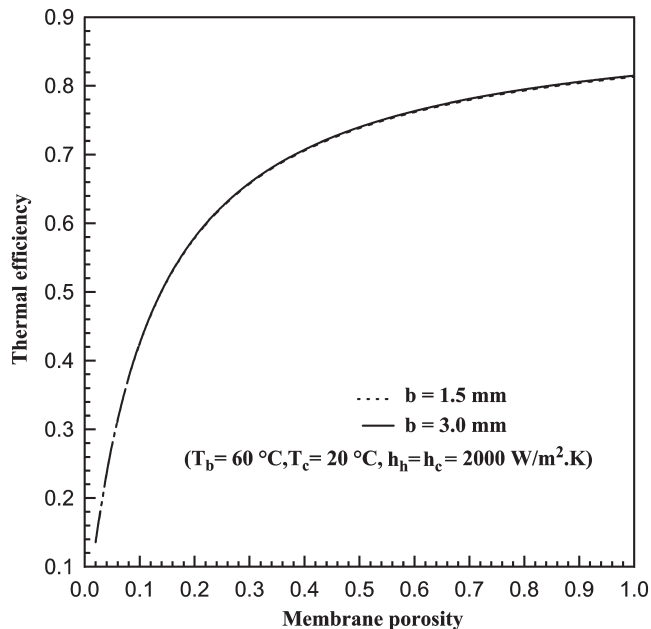


Figure 20. Effect of membrane porosity on thermal efficiency.

CONCLUSIONS

The sensitivity of the total mass flux in DCMD has been analyzed theoretically using different approaches for pure water system, the case similar to desalination. The analysis showed that temperature polarization may be reduced significantly by increasing the film heat transfer coefficients, h_h and h_c , which practically can be accomplished by increasing the velocities of the liquid streams. Temperature polarization can also be reduced by increasing the membrane thickness and decreasing the membrane porosity, however, a negligible small flux will be obtained in this case. On the other hand, the results showed that while the thermal efficiency increases with increasing h_h , it decreases with increasing h_c . Thus, to maximize the water production with commercially available membranes, attention should be directed towards a good module design to provide a high liquid film heat transfer coefficient in the hot side.

The analysis showed that the mass flux is highly sensitive to the bulk temperatures in comparison with other parameters. The sensitivity of the bulk temperatures becomes higher and higher as the bulk temperatures approach

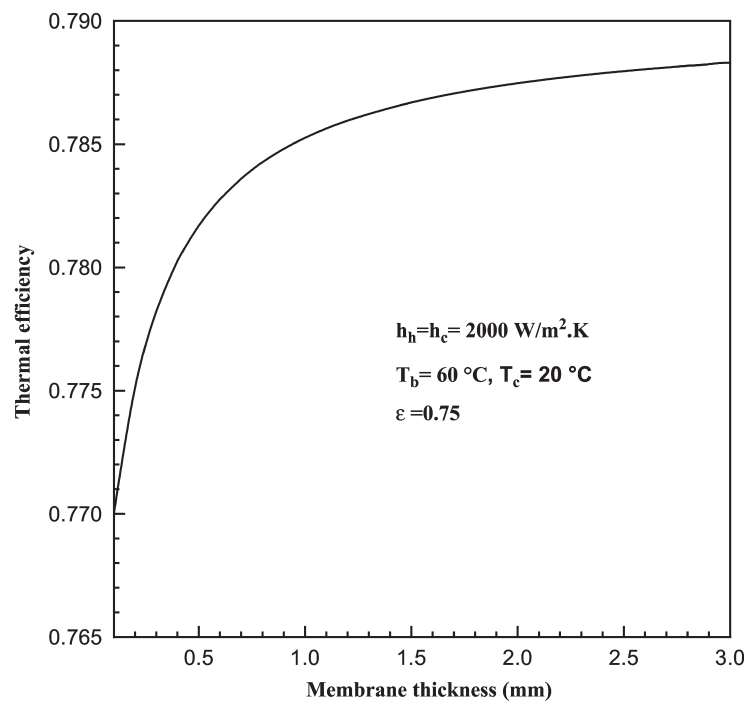


Figure 21. Effect of membrane thickness on thermal efficiency.

each other; when the bulk temperatures approach each other, a negligible small permeate flux is obtained and, correspondingly, an extremely high sensitivity is obtained, formally represented by a diverging value of the sensitivity factors.

NOMENCLATURE

<i>b</i>	membrane thickness (m)
<i>c</i>	molar concentration (mol/m ³)
<i>C_P</i>	heat capacity (J/kg K)
<i>D</i>	diffusion coefficient (m ² /sec)
<i>h</i>	heat transfer coefficient (W/m ² K)
<i>N</i>	mass flux (kg/m ² sec)
<i>P</i>	total pressure (N/m ²)
<i>q</i>	heat flux (W/m ²)



<i>R</i>	universal gas constant (J/mol K)
<i>S</i>	normalized sensitivity parameter
<i>T</i>	temperature (K)
<i>y</i>	mole fraction in the vapor phase
<i>z</i>	distance (m)
η	thermal efficiency
θ	temperature polarization factor
λ	latent heat of vaporization (J/kg)
ε	porosity
τ	tortuosity

REFERENCES

1. Findley, M. Vaporization Through Porous Membranes. *Ind. Eng. Chem. Process Des. Dev.* **1967**, *6*, 226–230.
2. Gostoli, C.; Sarti, G.C. Separation of Liquid Mixtures by Membrane Distillation. *J. Membr. Sci.* **1989**, *41*, 211–224.
3. Cheng, D.Y. Method and Apparatus for Distillation, United States Patent US 4,265,713, 1981.
4. Cheng, D.Y.; Wiersma, S.J. Composite Membranes for a Membrane Distillation System, United States Patent US 4,316,772, 1989.
5. Sarti, G.C.; Gostoli, C.; Matulli, S. Low Energy Cost Desalination Process Using Hydrophobic Membranes. *Desalination* **1985**, *56*, 277–286.
6. Sarti, G.C.; Gostoli, C. Use Hydrophobic Membranes in Thermal Separation of Liquid Mixtures: Theory and Experiments. In *Membrane and Membrane Processes*; Drioli, E., Nakagaki, M., Eds.; Plenum Press: New York, 1986; 349–360.
7. Sarti, G.C.; Gostoli, C.; Matulli, S. Low Temperature Distillation Through Hydrophobic Membranes. *Sep. Sci. Technol.* **1987**, *22*, 855–872.
8. Gostoli, C.; Sarti, G.C. Thermally Driven Mass Transport Through Membranes. In *Synthetic Polymeric Membranes*; Sedlacek, B., Kahovec, J., Eds.; Walter de Gruyter and Co.: Berlin, 1987; 515–529.
9. Fane, A.G.; Schofield, R.W.; Fell, C.J.D. The Efficiency Use of Energy in Membrane Distillation. *Desalination* **1987**, *64*, 231–243.
10. Banat, F.A.; Abu Al-Rub, F.A.; Jumah, R.; Shannag, M. On the Effect of Inert Gases in Breaking the Formic Acid–Water Azeotrope by Gas Gap Membrane Distillation. *J. Chem. Eng.* **1999**, *73*, 37–42.
11. Banat, F.A.; Abu Al-Rub, F.A.; Jumah, R.; Shannag, M. Theoretical Investigation of Membrane Distillation Role in Breaking the Formic Acid–Water Azeotropic Point: Comparison Between Fickian and Stefan-



Maxwell-Based Models. *Int. Comm. Heat Mass Transfer* **1999**, *26*, 879–888.

- 12. Banat, F.A.; Abu Al-Rub, F.A.; Jumah, R.; Shannag, M. Application of Stefan-Maxwell Approach to Azeotropic Separation by Membrane Distillation: Short Communication. *J. Chem. Eng.* **1999**, *73*, 71–75.
- 13. Banat, F.A.; Abu Al-Rub, F.A.; Jumah, R.; Shannag, M. Simultaneous Removal of Acetone and Ethanol from Aqueous Solutions by Membrane Distillation: Prediction Using the Fick's and the Exact and Approximate Stefan-Maxwell Relations. *J. Heat Mass Transfer* **1999**, *35*, 423–431.
- 14. Abu Al-Rub, F.A.; Banat, F.A.; Shannag, M. Theoretical Assessment of Dilute Acetone Removal from Aqueous Streams by Membrane Distillation. *Sep. Sci. Technol.* **1999**, *34*, 2817–2836.
- 15. Bandini, S.; Gostoli, C.; Sarti, G.C. Role of Heat and Mass Transfer in Membrane Distillation Process. *Desalination* **1991**, *81*, 91–106.
- 16. Banat, F.A.; Abu Al-Rub, F.A.; Beni-Melhim, K. Desalination by Vacuum Membrane Distillation: Sensitivity Analysis, Collaborative Research in Eastern Mediterranean (EMCC-2), Ankara, Turkey, May 20–24, 2001.
- 17. Bird, R.B.; Stewart, W.E.; Lightfoot, E.N. *Transport Phenomena*; Wiley: New York, 1960.
- 18. Miguel, A.; Jose, M.; Fernanda, S.; Rosa, N.; Julia, S. Application of Parametric Sensitivity Analysis to Batch Process Safety: Theoretical and Experimental Studies. *Chem. Eng. Technol.* **1996**, *19*, 222–232.

Received June 2001

Revised November 2001